Biochimica et Biophysica Acta 1828 (2013) 1094–1101

Contents lists available at SciVerse ScienceDirect

Biochimica et Biophysica Acta

journal homepage: www.elsevier.com/locate/bbamem

# Sensing hydration and behavior of pyrene in POPC and POPC/cholesterol bilayers: A molecular dynamics study

Luís M.S. Loura [a,b,*], António M.T. Martins do Canto [c,d], Jorge Martins [e,f,**]

[a] Faculdade de Farmácia, Universidade de Coimbra, Pólo das Ciências da Saúde, Azinhaga de Santa Comba, 3000-548 Coimbra, Portugal
[b] Centro de Química de Coimbra, Largo D. Dinis, Rua Larga, 3004-535 Coimbra, Portugal
[c] Departamento de Química, Escola de Ciências e Tecnologia, Universidade de Évora, Rua Romão Ramalho, 59, 7000-671 Évora, Portugal
[d] Centro de Química de Évora, Universidade de Évora, Rua Romão Ramalho, 59, 7000-671 Évora, Portugal
[e] IBB–CBME, Universidade do Algarve, Campus de Gambelas, 8005-139 Faro, Portugal
[f] DCBB–FCT, Universidade do Algarve, Campus de Gambelas, 8005-139 Faro, Portugal

ARTICLE INFO

*Article history:*
Received 6 October 2012
Received in revised form 12 December 2012
Accepted 18 December 2012
Available online 26 December 2012

*Keywords:*
Fluorescent membrane probe
Ham effect
Lipid bilayer
Molecular dynamics simulation
Pyrene
*Py* polarity scale

ABSTRACT

Molecular dynamics (MD) simulations of bilayers of 1-palmitoyl-2-oleoyl-*sn*-glycero-3-phosphocholine (POPC) with varying amounts of cholesterol (0, 5, 20, and 40 mol%) were carried out in the absence and presence of inserted pyrene molecules. Both fluorophore and bilayer parameters were computed, for characterization of probe location and dynamics, as well as its effects on the host bilayer. In agreement with previous studies in fluid disordered bilayers, pyrene prefers to be located in the hydrophobic acyl chain region of POPC bilayers, close to the glycerol group of lipid molecules and causes ordering of the lipid acyl chains. However, incorporation of pyrene in binary POPC/cholesterol bilayers decreases the acyl chain order parameter (especially near the end of the chains), opposing the ordering effect of cholesterol. These effects are modest and mainly felt locally. Significantly, as the bilayer is enriched with cholesterol, the relative position of pyrene and the POPC carbonyl and phosphocholine groups is invariant, and the local water density around the probe decreases. This work clarifies and supports the cautious use of pyrene Ham effect to effectively measure equivalent polarity in lipid bilayers. Within the time scale of the MD simulations, which is of the magnitude of the fluorescence lifetime of pyrene, the thermally averaged polarity of lipid bilayers is nearly out of influence of spurious uncertainty in the transverse location of pyrene in the bilayers. This renders the values of equivalent polarity measurements through the pyrene Ham effect more reliable and reproducible than previously expected.



## 1. Introduction

The characterization of the structure, dynamics and functioning of biomembranes at the molecular level requires the use of numerous complementary biophysical techniques, both experimental and theoretical. Among the former, fluorescence spectroscopy is especially important, owing to its very high sensitivity and versatility. However, most fluorescence studies of lipid bilayers require extrinsic probes, which behavior and potential perturbing effects are often unclear. To this end, molecular dynamics (MD) simulations have been established as a useful method for the characterization of lipid membrane systems (see, *e.g.*, the recent review by Lyubartsev and Rabinovich [1] and references therein) and, in particular, to realize the behavior of fluorescence probes upon incorporation in lipid bilayers [2,3].

Pyrene is a polycyclic aromatic hydrocarbon noted for its remarkable spectroscopic properties, such as an unusually long fluorescence lifetime (>100 ns in a variety of aerated solvents and membrane systems), emission spectrum highly sensitive to solvent polarity and concentration-dependent and/or viscosity-dependent excimer formation. Due to these distinctive features, both free pyrene and pyrene-labeled lipids have been used as probes in membrane biophysics studies [4,5]. Concerning free pyrene, two MD studies reports have been published. The first combined MD and deuterium NMR measurements [6]. The simulated system consisted of 128 molecules of 1-palmitoyl-2-oleoyl-*sn*-glycero-3-phosphocholine (POPC), with four pyrene molecules inserted inside the membrane and a fifth located in the water region of the box at the start of the MD run, which spanned 25 ns. The latter pyrene molecule was found to partition into and inserting the POPC bilayer rapidly (<2 ns). Within ~8 ns of the start, all five molecules were located slightly inside the

*Abbreviations:* DPPC, 1,2-dipalmitoyl-*sn*-glycero-3-phosphocholine; MD, molecular dynamics; POPC, 1-palmitoyl-2-oleoyl-*sn*-glycero-3-phosphocholine; RDF, radial distribution function

* Correspondence to: L.M.S. Loura, Faculdade de Farmácia, Universidade de Coimbra, Pólo das Ciências da Saúde, Azinhaga de Santa Comba, 3000-548 Coimbra, Portugal. Tel.: +351 239488485; fax: +351 239827126.
** Correspondence to: J. Martins, IBB–CBME, Universidade do Algarve, Campus de Gambelas, 8005-139 Faro, Portugal. Tel.: +351 289800900; fax: +351 289800066.
*E-mail addresses:* lloura@ff.uc.pt (L.M.S. Loura), jmartin@ualg.pt (J. Martins).

0005-2736/$ – see front matter © 2012 Elsevier B.V. All rights reserved.
http://dx.doi.org/10.1016/j.bbamem.2012.12.014

headgroup region of the bilayer. This somewhat shallow location agrees with published experimental fluorescence quenching reports [7,8] and could be due to entropic reasons, as location of this apolar, large and rigid molecule in the highly disordered middle region of the bilayer, would imply considerable acyl-chain ordering and entropy decrease. No flip-flops were observed during the time-scale of the simulations. The molecules were found to have their long axis essentially aligned (within ~30°) with the bilayer normal. Good agreement between probe order parameter values determined from deuterium NMR and MD was verified, seemingly indicating that even 25 ns of simulation appeared to be enough to cover all types of motions that pyrene performs inside a lipid bilayer.

The second study was carried out in both fluid ($T=325$ K or 350 K, 20 ns) and gel 1,2-dipalmitoyl-*sn*-glycero-3-phosphocholine (DPPC; $T=273$ K, 50 ns) bilayers [9]. For all systems, the overall effects of pyrene on area/lipid and deuterium order parameter ($-S_{CD}$) are minor. However, significant local (for lipid-closest probe distances $R<1.0$ nm) effects are present. In the fluid phase simulations, acyl chain ordering is verified. Concerning the gel phase, analysis of $-S_{CD}$ is rendered difficult because pyrene reduces the tilt angle of nearby DPPC acyl chains, which would *per se* result in an increased order parameter (as the latter reflects the angle between the chain and the bilayer normal). However, the fraction of *trans*/*gauche* defects along the acyl chains of neighboring DPPC molecules actually increases, meaning that pyrene molecules decrease their ordering. Variations of bilayer thickness are consistent with these findings, and pyrene incorporation causes a significant reduction and minor increase in the gel and fluid phases, respectively. Pyrene has broad transverse distribution and orientation profiles, with maxima around acyl chain carbon 5 (distribution) and for $\theta=90°$ (orientation of the pyrene plane relative to the bilayer plane), respectively. Both observations are in agreement with Hoff et al. [6]. In the gel phase, the orientation profile is slightly more complex, with a second maximum being apparent at 50° (probably reflecting the tilt of the DPPC acyl chains). No significant changes in lateral diffusion coefficient of DPPC were observed upon pyrene insertion. No clustering of pyrene molecules was observed, possibly as a result of time scale limitations.

In the present work, pyrene MD simulation is carried out in pure POPC and mixed POPC/cholesterol bilayers containing variable amounts (5, 20, and 40 mol%) of the sterol component (cholesterol), and thus presenting variable extents of phospholipid acyl chain order, ranging from the liquid-disordered phase to the predicted liquid-ordered phase. Emphasis is given to the degree of proximity between the pyrene fluorophore and water molecules inside bilayers, in order to gain insights on the measurement of equivalent lipid bilayer polarity through the pyrene Ham effect [10]. The empirical *Py* polarity scale is an independent and robust descriptor of the lipid membrane polarity through the dipolarity/polarizability mode of mutual interactions between pyrene and the complex composite lipid bilayer molecular environment, determined mainly by the extent of hydration within the hydrophobic core of bilayers. The *Py* polarity scale is based on the measurement of the ratio of the fluorescence intensities of the first and third vibronic bands ($I_1/I_3$) in the pyrene emission spectra (see [10] and references therein). Due to the remarkable sensitivity of fluorescence techniques, the *Py* scale is extremely responsive to solvent polarity, because $I_1$ corresponds to a symmetry forbidden electronic transition, which depends on the polarity of the medium, while $I_3$ is assigned to a transition nearly independent on polarity (being this way a calibrating parameter for the calculated $I_1/I_3$ ratio). However, doubts can be raised concerning the average precise location of the free pyrene molecule inside bilayers (liberated transversal movements were early forecast [11]), and whether or not this probe introduces overlooked perturbations in membrane structure and/or dynamics. Both issues can even be potentially magnified in bilayers containing phospholipid/cholesterol mixtures, along with the observed and quantified variations in the hydration of these lipid bilayers [10]. We present a detailed and relatively extensive analysis of the pyrene location, proximity to water molecules, and of the effects on the structure and dynamics of lipid bilayers composed by pure POPC and various mixtures with cholesterol. The thermally averaged location is in accordance with the findings obtained through varied experimental techniques (X-ray diffraction, NMR and fluorescence) and other MD simulation studies [6–9,12]. The interaction of pyrene with water molecules inside the lipid bilayers shows that the hydration of POPC bilayers does depend on the proportion of cholesterol, the equivalent polarity decreasing with the cholesterol content [13]. The presumed effects of the pyrene in the bilayer structure and dynamics are small, even for relatively large molar proportion of pyrene probe used in these atomic-level simulations (1.56 mol% and 3.13 mol%), and the impacts of the cholesterol content in the average location of pyrene molecules, inside both pure and mixed bilayers, are revealed as being nearly negligible. It is also worth to highlight that although the present MD simulations consider the pyrene molecules solely in the ground state, and the experimental data counterpart is obtained from the excited state fluorescence emission, the general accordance of both outcomes is quite remarkable. That is to say that within an analogous time resolution of both type of approaches (100 ns in the present MD simulations, and more than 100 ns in the experimental fluorescence measurements), the averaged local density of water inside lipid bilayers is unequivocally matching. In both cases, the equivalent polarity or the local water density is being averaged in two planes: the transverse dimension of bilayers, due to the molecular dimensions of pyrene itself (sensing different chemical environments within the $\approx$1 nm of the pyrene long axis) as well as small-scale up-and-down motions, and in the two-dimensional bilayers plane, due to the lateral diffusion of lipid membrane components during the pyrene excited-state lifetime (also sensing different chemical environments, corresponding to several two-dimensional diffusive steps of free pyrene molecules in the bilayers). Additionally, in both approaches the molecular rotational diffusion dynamics (for amphiphiles such as POPC and cholesterol, and for apolar pyrene) is operating and exerting the corresponding influences in the outcomes, within an analogous time frame, e.g. the rotational dynamics (rotational correlation time lower than 10 ns) is averaging the transverse differential polarity from the interface to the apolar center of bilayers, at least along the $\approx$1 nm longest dimension of the pyrene molecule itself.

## 2. Simulation details

MD simulations and analysis of trajectories was carried out using the GROMACS 3.3.3 package [14,15]. The SPC water model was used [16]. The topology of the POPC molecule (using a united united-atom description for CH, $CH_2$, and $CH_3$ groups, based on the parameters presented by Berger et al. [17] for 1,2-dipalmitoyl-*sn*-glycero-3-phosphocholine (DPPC), together with the coordinate file of a POPC bilayer, was obtained from Dr. Peter Tieleman's group webpage (http://moose.bio.ucalgary.ca/index.php?page=Structures_and_Topologies) [6]. One POPC molecule from the downloaded POPC bilayer coordinate file was used to build a fully hydrated (3902 water molecules) 128-lipid bilayer using GROMACS model set-up programs. Cholesterol model molecules and their bonded and non-bonded parameters were taken from Holtje et al. [18] and were downloaded from the GROMACS web page (http://www.gromacs.org/index.php?title=Download_%26_Installation/User_contributions/Molecule_topologies), whereas pyrene was parameterized as described by Hoff [6,19]. Bilayers containing 5 mol%, 20 mol%, and 40 mol% cholesterol (152 POPC:8 cholesterol, 120 POPC:30 cholesterol, and 90 POPC:60 cholesterol, respectively) were built using GROMACS model preparation packages. Bilayers containing 2 or 4 pyrene molecules (one or two in each leaflet, respectively) were then obtained by randomly inserting probe molecules inside a POPC or POPC/cholesterol bilayer without replacement of lipids. Fig. 1 shows structures and numbering of relevant atoms of the POPC, cholesterol and pyrene molecules.

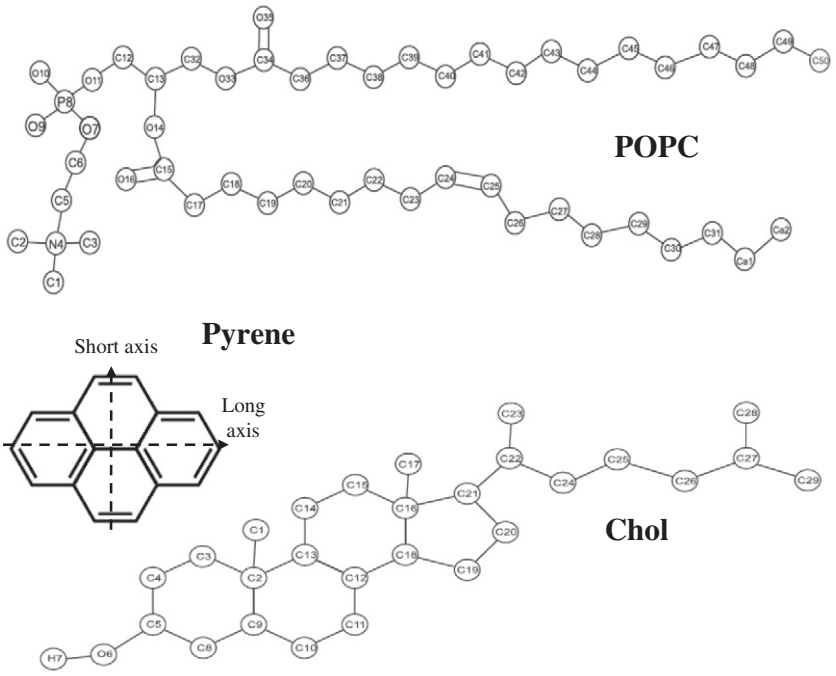


**Fig. 1.** Structures of POPC, cholesterol and pyrene. Atom numbering for POPC and cholesterol, as mentioned throughout the text, is also shown.

In all systems, unfavorable atomic contacts were removed by steepest descent energy minimization. For each system, a short (100 ps) MD run was then carried out using a 1 fs integration step, followed by a 100 ns run using a 4 fs integration step. The use of this time step was made possible by constraining bond lengths and angles to their equilibrium values, using the SETTLE algorithm [20] for water and the LINCS algorithm [21] for all other bonds (see also discussion in [22,23]). All simulations were carried out under constant number of particles, pressure (1 bar) and temperature (298.15 K), and with periodic boundary conditions. Pressure and temperature control were carried out using the weak-coupling Berendsen schemes [24], with coupling times of 1.0 ps and 0.1 ps, respectively. Semi-isotropic pressure coupling was used. Van der Waals and Coulomb interactions were cut-off at 1.0 nm, whereas for long-range electrostatics the particle mesh Ewald treatment was applied [25]. While the use of a relatively small van der Waals cut-off without introducing long-range dispersion corrections (as done by Berger et al. [17]) has been observed to lead to more expanded and disordered bilayers (see *e.g.*, [23,26]), this is apparently not the case in our systems. In fact, our choice of parameters has been previously used in the simulation of POPC and POPC/cholesterol bilayers, with recovery of adequate values for average area/lipid and acyl chain order parameters [27–30]. The first 20 ns of each simulation were used for equilibration, and the remaining 80 ns were used for analysis. Errors were calculated according to the block method of Flyvbjerg and Petersen [31]. VMD software was used for visualization purposes [32].

## 3. Results and discussion

Fig. 2 shows final snapshots for simulations of 4 pyrene molecules in a disordered (0 mol% cholesterol, Fig. 2A) and in an ordered (20 mol% cholesterol, Fig. 2B) system. These configurations illustrate some of the essential features: as widely known, cholesterol induces ordering of the phospholipid acyl chains, whereas pyrene molecules locate below the phospholipid headgroups but stay far from the center of the bilayer. The pyrene molecule plane tends to align with the bilayer normal direction in the POPC/cholesterol system, but possesses a large degree of orientation freedom in pure POPC.

The time variation of the area per lipid is a common indicator of the equilibration of bilayer simulations (see *e.g.*, [33]), whereas its average value is often used to assess the adequacy of the simulation methodology, due to its sensitiveness to simulation details [23]. For one-component bilayers (such as the POPC system in the present work), the area per lipid is simply calculated as the area of the simulation box divided by the number of lipid molecules in each leaflet. For binary systems (such as POPC/cholesterol bilayers), evaluation of the area per each component is not a trivial issue. In this work, areas per POPC ($a_{POPC}$) and cholesterol ($a_{Chol}$) were calculated using the following equations [34]:

$$a_{POPC} = \frac{2A}{V - n_w v_w} \frac{V - n_w v_w - n_{Chol} v_{Chol}}{n_{POPC}} \quad (1)$$

$$a_{Chol} = \frac{2A v_{Chol}}{V - n_w v_w} \quad (2)$$

In these equations, $a_{POPC}$ and $a_{Chol}$ are the cross-sectional area per POPC and cholesterol molecules, $A$ and $V$ are the instant simulation box area (in the $xy$ plane, parallel to the bilayer) and volume, $n_w$ and $n_{POPC}$ are the number of water and POPC molecules in the simulation, and $v_w = 0.0312$ nm$^3$ and $v_{Chol} = 0.593$ nm$^3$ are the molecular volumes of water and cholesterol, respectively [34]. These equations implicitly assume that the area fractions of POPC and cholesterol are equal to their volume fractions, and their limitations have been discussed at length recently [35]. They are used here as they allow for simple verification of system equilibration as well as a semi-quantitative assessment (rather than precise calculation) of the condensing effect of cholesterol.

Fig. S1 depicts the time evolution of $a_{POPC}$ and $a_{Chol}$ for the systems under study, whereas Table 1 shows the average values. Our results for $a_{POPC}$ agree with the experimental values of 0.65 nm$^2$ ($T = 298$ K; Lantzsch et al. [36]), 0.64 nm$^2$ ($T = 298$ K; Konig et al. [37]), and 0.63 nm$^2$ ($T = 297$ K; Smaby et al. [38]), as well as with those obtained from MD simulations by Böckmann et al. [39] ($T = 300$ K, $a = 0.655$ nm$^2$), Mukhopadhyay et al. [40] ($T = 298$ K, $a = 0.62$ nm$^2$),

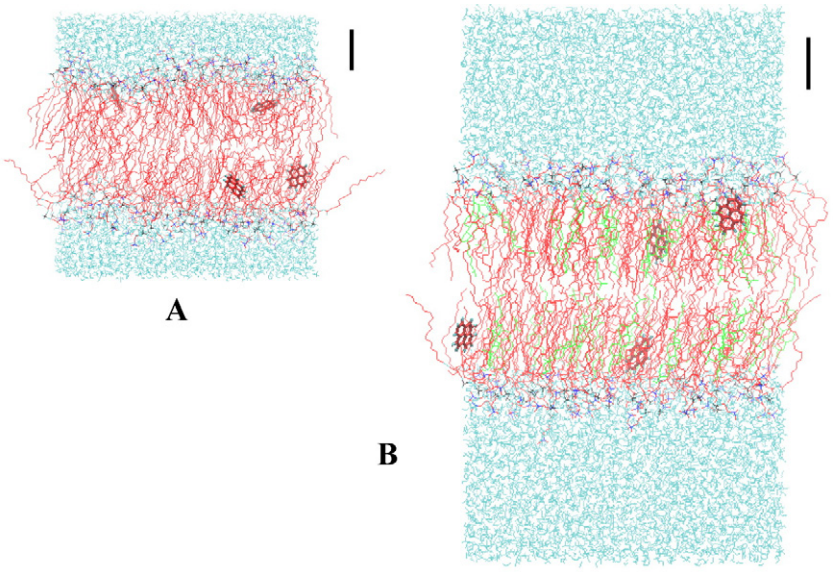


**Fig. 2.** Final snapshots of the 4-pyrene simulations for 0 (A) and 20 (B) mol% cholesterol systems. POPC $CH_n$ groups (n = 0–3), O atoms, N atoms, and P atoms are shown in red, cyan, blue and black, respectively. Water and cholesterol molecules are shown in cyan and bright green, respectively. Pyrene molecules are depicted in licorice drawing style. Scale bar length represents 1 nm in both panels.

Gurtovenko and Anwar [41] ($T = 310$ K, $a = 0.65$ nm$^2$), and Pandit et al. [42] ($T = 303$ K, $a = 0.63$ nm$^2$).

Mass density profiles were calculated for all components of the simulated systems, and are depicted in Fig. 3 for the bilayers with two inserted pyrene molecules. It is visible that whereas pyrene molecules are well inserted in the bilayer, their transverse distribution still presents some degree of overlap with that of water. This relatively shallow location of pyrene agrees with that verified in other MD studies [6,9].

This can also be assessed by looking at the average transverse location of selected atoms, as shown in Fig. S2. As seen in the figure, the center of mass of pyrene lies on average at a depth similar to that of the cholesterol ring system (between cholesterol atoms C5 and C16). By comparing the transverse location of POPC and cholesterol atoms for varying number of pyrene molecules, it is apparent that the effect of pyrene insertion is rather modest. Globally, pyrene seems to cause a minor increase of bilayer thickness in the disordered systems (0 and 5 mol% cholesterol) and conversely for the ordered ones (20 and 40 mol% cholesterol). However, the variations observed are mostly <2% and thus less than the uncertainty associated to these values (which is typically 3–4 mol%; data not shown).

Orientation of bilayer-inserted pyrene molecules was studied considering the long and short molecular axes defined in Fig. 1. Fig. 4 depicts the distributions of the angles between the long molecular axis, the short molecular axis and the normal to the molecule plane, relative to the bilayer normal. Note that due to the high symmetry of pyrene, there is two-fold orientation degeneracy of the represented angles. The apparent bimodal distribution of the long axis (with peaks at ~30° and ~150°) reflects this feature, which is not visible in the other distributions, due to their maxima being near ~90°. The preferential alignments of the long axis and the molecular plane in the directions of the bilayer normal and perpendicular to the latter, respectively, agree with previous simulation studies [6,9]. As the cholesterol content is increased, the angular distributions become somewhat narrower and better defined, reflecting the concomitant increase in order in the hydrophobic region of the bilayer.

Whereas pyrene orientation is largely modulated by the bilayer composition, membrane order is conversely affected by the presence of pyrene molecules. This was hinted at but barely noticeable in the modest variations in bilayer thickness (Fig. S2) but is clearly noticeable in the deuterium order parameter $-S_{CD}$. In our simulations, using a united atom force field, $S_{CD}$ for saturated ($S_{CD}^{sat}$) and unsaturated ($S_{CD}^{unsat}$) carbons is determined using the following relations [43]:

$$-S_{CD}^{sat} = \frac{2}{3}S_{xx} + \frac{1}{3}S_{yy} \tag{3}$$

$$-S_{CD}^{unsat} = \frac{1}{4}S_{zz} + \frac{3}{4}S_{yy} + \frac{\sqrt{3}}{2}S_{xy} \tag{4}$$

where $S_{ab}$ are the order tensor coordinates, given by

$$S_{ab} = \frac{1}{2}\langle 3\cos\theta_a 3\cos\theta_b - \delta_{ab}\rangle \qquad a,b = x,y,z \tag{5}$$

where in turn $\theta_a$ (or $\theta_b$) is the angle made by $a$th (or $b$th) molecular axis with the bilayer normal and $\delta_{ab}$ is the Kronecker delta (<> denotes both ensemble and time averaging).

**Table 1**
Average areas/molecule for the different simulated systems.

| | Number of inserted pyrene molecules | | | | | |
|---|---|---|---|---|---|---|
| | 0 | | 2 | | 4 | |
| mol% Chol | $a_{POPC}$/nm$^2$ | $a_{Chol}$/nm$^2$ | $a_{POPC}$/nm$^2$ | $a_{Chol}$/nm$^2$ | $a_{POPC}$/nm$^2$ | $a_{Chol}$/nm$^2$ |
| 0 | 0.625 ± 0.015 | – | 0.622 ± 0.019 | – | 0.626 ± 0.020 | – |
| 5 | 0.614 ± 0.016 | 0.296 ± 0.008 | 0.611 ± 0.015 | 0.293 ± 0.007 | 0.610 ± 0.016 | 0.293 ± 0.008 |
| 20 | 0.534 ± 0.015 | 0.265 ± 0.007 | 0.543 ± 0.015 | 0.267 ± 0.007 | 0.550 ± 0.014 | 0.270 ± 0.007 |
| 40 | 0.511 ± 0.013 | 0.259 ± 0.007 | 0.509 ± 0.014 | 0.258 ± 0.007 | 0.524 ± 0.014 | 0.263 ± 0.007 |

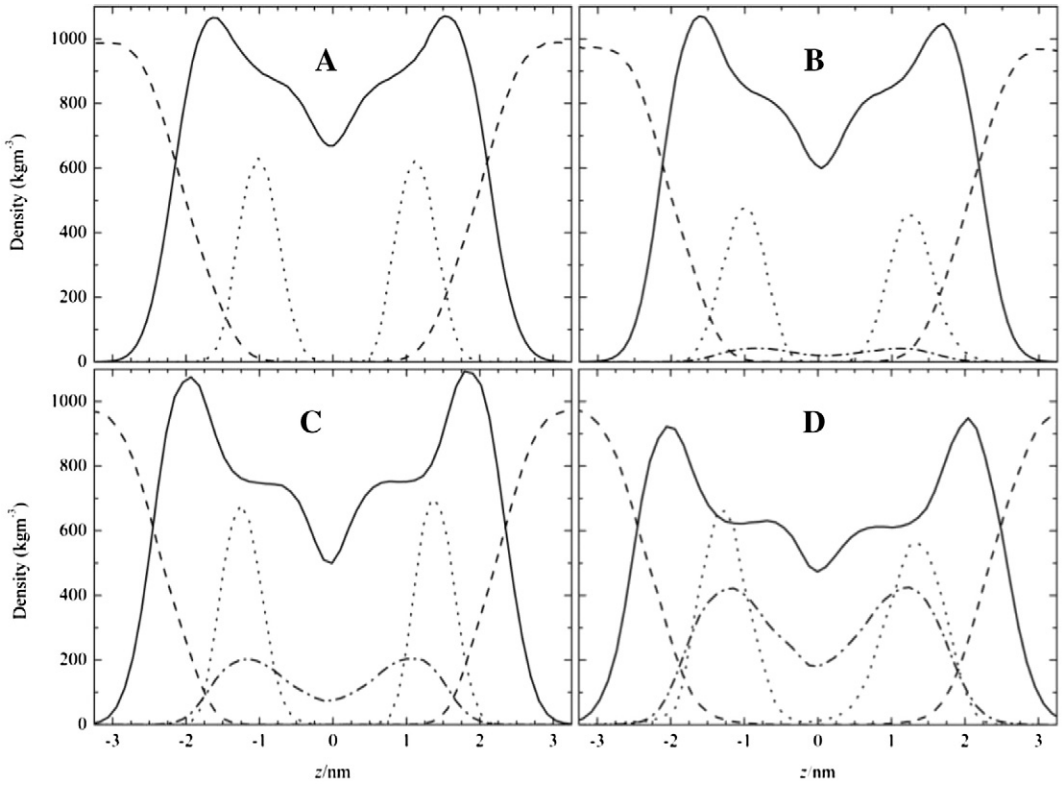


**Fig. 3.** Mass density profiles (solid: POPC; dash: water; dot: pyrene multiplied by 50; dot-dash: cholesterol) for bilayers with two inserted pyrene molecules (A: 0 mol% cholesterol; B: 5 mol% cholesterol; C: 20 mol% cholesterol; D: 40 mol% cholesterol).

$-S_{CD}$ can vary between 0.5 (full order along the bilayer normal) and −0.25 (full order along the bilayer plane), whereas $S_{CD}=0$ denotes isotropic orientation. Due to the slow convergence of this parameter [44], analysis was restricted to the last 25 ns of the simulations. Order parameters were calculated for both acyl chains of POPC (Fig. 5). For pure phospholipid bilayer, the profiles obtained agreed with both experimental (e.g., [45,46]) and simulated (e.g., [39,41,47,48]) data. Incorporation of pyrene leads to small but noticeable effects on $-S_{CD}$ of both acyl chains, namely order increase in pure POPC and decrease in POPC/cholesterol. The latter effect is more significant near the end of the acyl chain (from the 10th C atom onwards) and can be understood by noting that whereas pyrene has a rigid structure stemming from its polycyclic ring system, its distribution does not span the $|z|<0.5$ nm region of the bilayer (see mass profiles of Fig. 3). Hence, incorporation of a pyrene molecule in a given location creates free volume directly underneath it, which may be occupied by ends of neighbouring POPC acyl chains. This leads to a local reduction of the acyl chain order parameter in this region. This behavior is in contrast with cholesterol, which, via its side chain, is able to occupy the center of bilayer (Fig. 3).

These effects are most noticeable if $-S_{CD}$ is calculated as a function of the distance to the closest pyrene molecule in the same bilayer leaflet, $R$, as illustrated in Fig. 6 for pure POPC and POPC/20 mol% cholesterol [3]. In pure POPC, pyrene induces considerable ordering in nearby ($R<0.6$ nm) POPC acyl chains up to the 10th C atom. Closer to the end of the chain, the effect is much weaker for the reasons given above. Switching to the POPC/cholesterol bilayer, it can be seen that pyrene insertion leads to a small but already noticeable decrease in the order parameter of the first C atoms of the POPC acyl chains at short range. As one moves along the chain, this disordering effect becomes much more pronounced. Overall, one may conclude that whereas pyrene effects on POPC acyl chain order parameters are rather small in global terms, significant changes are felt locally.

This trend of inducing ordering of nearby phospholipid chains in disordered phases and conversely for ordered bilayer systems can be observed in other properties, such as tilting of the cholesterol molecule (pyrene increases the average tilt of cholesterol long axis, whereas it does not affect orientation of the P–N axis of POPC, Table S1), as well as lateral and rotational diffusion of the bilayer components (pyrene generally increases rotational tumbling of molecular vectors in POPC/

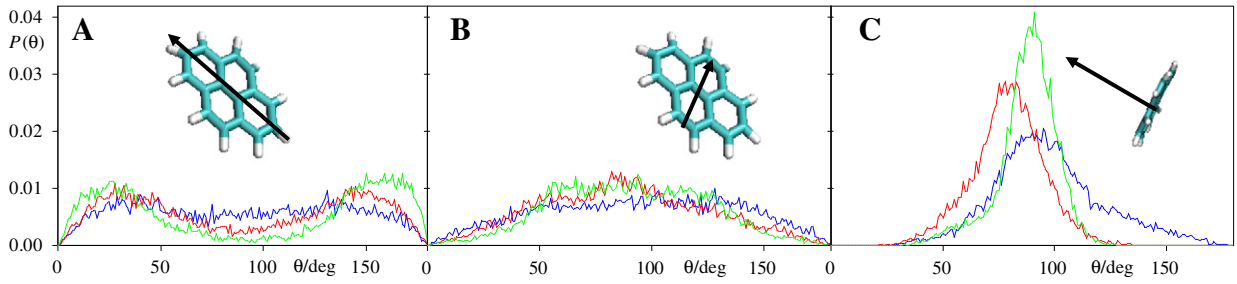


**Fig. 4.** Probability density functions $P(\theta)$ of the angles between the long axis (A), the short axis (B), and the normal to the pyrene plane (defined as the vector product of the short and long axes; C), relative to the bilayer normal. Blue, red and green lines refer to the 0 mol%, 20 mol% and 40 mol% cholesterol systems, respectively.

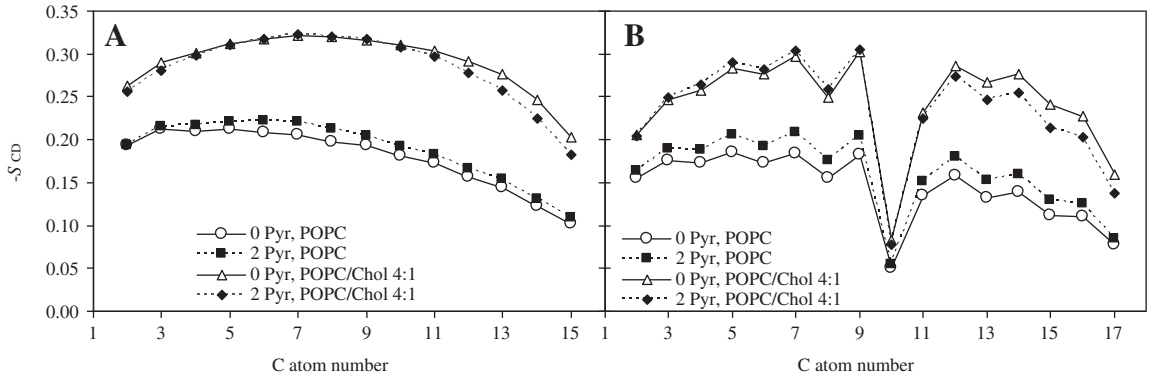


**Fig. 5.** Deuterium order parameter $-S_{CD}$ calculated for the *sn*-1 (A) and *sn*-2 (B) POPC acyl chains in the POPC and POPC/cholesterol (20 mol% cholesterol) systems, in the presence of either none or two pyrene molecules.

cholesterol 20 mol%, decreases lateral mobility of POPC in the absence of cholesterol, and increases lateral mobility of both POPC and cholesterol in POPC/cholesterol 20 mol%; see Figs. S3 and S4).

Turning now our attention to the interaction between pyrene and water molecules, radial distribution functions (RDFs) of water around pyrene, $g(r)$, were calculated and are shown in Fig. 7 for the 2 pyrene simulations.

Because the bulk density of water molecules is essentially invariant (equal to the value for pure water, $\rho = 33.3\ nm^{-3}$ at 298 K), $g(r)$ is proportional to the local number density of water at a distance $R$ to a pyrene molecule. It is clear that, for a given $R$ value, as the cholesterol content increases in the bilayer, the local density of water decreases, and thus pyrene molecules "sense" less water in their vicinity.

A preliminary survey on the experimental measurements of the lipid bilayer polarity of multilamellar vesicles composed of pure POPC and POPC/cholesterol mixtures from 5 mol% to 45 mol% of cholesterol appeared elsewhere [13], and those groundwork findings are in generic agreement with the results presented in the present MD simulations. Briefly, the equivalent polarity measured through the pyrene Ham effect shows a dependence on the proportion of cholesterol in the mixed POPC/cholesterol bilayers, being higher for pure POPC and low cholesterol content (up to 30 mol%) and lowering for high cholesterol content (data not shown). Therefore, the present study reinforces the experimental studies on the measurement of equivalent lipid bilayer polarity in model membranes containing unsaturated phosphatidylcholines, such as POPC, and cholesterol. Those quantitative studies are unequivocally meaningful, since the precise average location of the pyrene probe inside the bilayer is corroborated by the measured values for the equivalent lipid bilayer polarity in the identical model membrane system, and in addition, there are barely any artefacts regarding this location as a function of the cholesterol content in those lipid bilayers. The average transverse distance of pyrene to the bilayer midplane increases as the bilayer becomes enriched in cholesterol (Fig. S2). This occurs because of the overall increase in bilayer thickness induced by Chol, and, in fact, the relative position of pyrene and the POPC carbonyl and phosphocholine groups is invariant, as clearly illustrated in the unchanged locations of the water RDF maxima (due to H-bonding to these POPC moieties) around pyrene (Fig. 7).

In Fig. 7, it can also be seen that the density of water molecules in the vicinity of the pyrene molecules is generally decreasing from pure POPC to the mixture containing 40 mol% of cholesterol. Some additional details should be highlighted. There is an increased number of water molecules at a distance of $\approx 0.65$ nm and at $\approx 1.05$ nm, and these peaks can be assigned to the maxima of transbilayer profile of volume densities [49] corresponding to water molecules bonded to the phospholipids' carbonyls and to the phosphocholine groups, respectively. Taking as reference the water molecules hydrogen-bonded to carbonyls and to phosphates, the distance from the center of mass of pyrene molecules is invariant within the thermally averaged movements of both the pyrene and lipid molecules: the peak corresponding to the carbonyls shows a half-width of $\approx 1$ nm, and the peak of phosphate an analogous half-width of $\approx 2$ nm. Both results are consistent with the thermal motions characteristic of these groups, e.g. the phosphocholine group is more mobile than the carbonyls. However, there is an inversion of the number of water molecules in the vicinity of pyrene for pure POPC and the 5 mol% cholesterol mixture. At the distance of $\approx 0.65$ nm, there are less water molecules for pure POPC than for 5 mol% cholesterol. This sole off-trend result (not observed in the 4 pyrene simulations, not

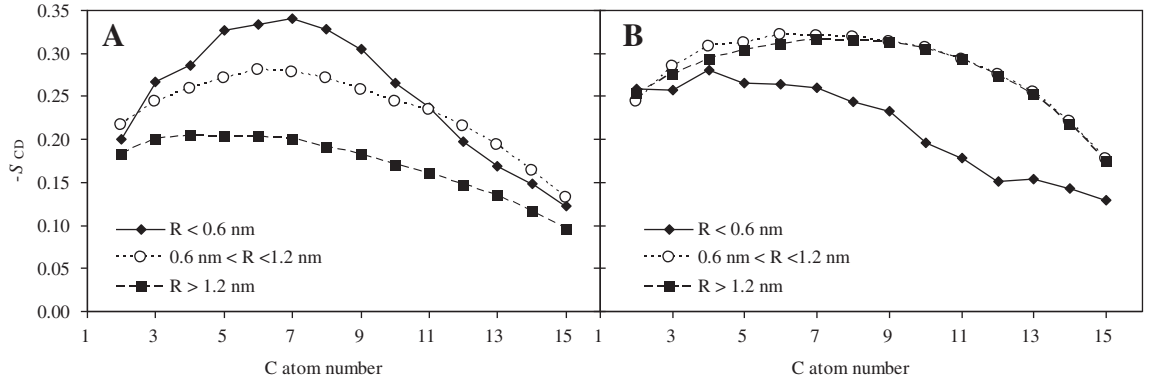


**Fig. 6.** Deuterium order parameter $-S_{CD}$ of POPC *sn*-1 acyl chain for varying distance to the closest pyrene molecule in the same bilayer leaflet, $R$, in the POPC (A) and POPC/cholesterol (20 mol% cholesterol; B) systems, in the presence of two pyrene molecules [3].

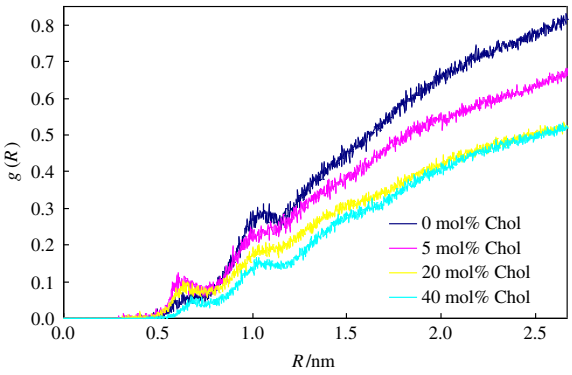


**Fig. 7.** Radial distribution functions $g(R)$ of water around the center of mass of pyrene, for bilayers of varying composition containing two probe molecules.

shown) is probably not significant and caused by sampling limitations imposed by the low probe content in the simulated systems.

Beyond this region, and up to $R \sim 2.0$ nm, RDFs begin to reflect contribution from "bulk" water. For the 0 and 5 mol% cholesterol systems, $g(R)$ approaches more rapidly the bulk value of unity, because of two combined effects: the higher density of water inside these bilayers (concomitant with a lower lipid density), and their smaller thickness (implying a larger relative contribution of "bulk" water to the RDF). For even larger distances ($R > 2.0$ nm), $g(R)$ is dominated by "bulk" water, and the different curves approach asymptotically unity in an essentially parallel way.

In Fig. 7, it is unequivocally shown that the local number density of water molecules around the pyrene molecules is effectively decreasing from pure POPC to the 20 and 40 mol% cholesterol systems, the latter showing identical water density profiles, within the experimental error. The diminished water density as a function of cholesterol in the bilayer is consistent with the observed decrease in the equivalent polarity measured through pyrene Ham effect in the very same model membrane system. The increased proportion of cholesterol in mixed POPC membranes produces a sort of dehydration in the lipidic bilayers.

## 4. Concluding remarks

In this work we use MD to simulate bilayers composed of varying proportions of POPC and cholesterol, spanning from 0 to 40 mol% of the latter. In agreement with recent results reported for DPPC above the gel/fluid transition temperature (Curdová et al., 2007), it is found that pyrene prefers to be located in the hydrophobic acyl chain region close to the glycerol group of lipid molecules and causes ordering of the lipid acyl chains in fluid disordered POPC bilayers. On the other hand, and similarly to one-component DPPC gel bilayers [9], incorporation of pyrene in binary POPC/cholesterol bilayers produces a disordering effect, increasing the area/lipid molecule and decreasing the bilayer thickness and acyl chain order parameter, and thus opposing the ordering effect of cholesterol. That is, even though pyrene, as a rigid planar molecule, induces ordering of nearby phospholipid acyl chains in disordered bilayers, it does so not as efficiently as cholesterol, and incorporation of pyrene in cholesterol-rich membrane systems leads to a disordering effect.

For the relatively extended time frame (100 ns) of the present MD simulations, enough to parallel with the experimental counterpart by using the pyrene fluorophore during its excited lifetime, there are no signs of other putative and relevant perturbations introduced by the probe to the structure and/or dynamics of the lipid bilayers, nor are there indications of other potential influences of the lipidic compositions of bilayers in the probe's behavior. The present simulations do not rule out other potentially relevant pyrene-related effects, such as aggregation of pyrene molecules and/or transversal movements of lipidic and probe molecules between the apposed monolayers (flip-flop), since these phenomena would fall out the 100 ns timescale. On the other hand, for the more ordered systems (20 mol% and 40 mol% cholesterol), the slower dynamics might affect the sampling efficiency, particularly in parameters concerning relatively rare events. This is the case for the order parameters and RDFs of neighboring ($R < 0.6$ nm to the closest pyrene) POPC molecules, since these constitute a minor fraction (~1–2%) of total lipid conformations. For these reason, these properties should be viewed more cautiously.

In any case, this does not distract from our overall conclusions. The present work offers a long standing required enlightenment on the presumed effects of the free pyrene fluorescent probe in the structure and dynamics of lipid model membranes, in particular for those containing cholesterol. Additionally, the presumed effects of the lipidic composition of the mixed cholesterol bilayers in the transverse location of pyrene have been clarified. In both cases, the effects are practically negligible for the purposes of rendering meaningful and self-consistent the experimental measurements of equivalent polarity in homologous lipid bilayers systems.

## Acknowledgements

L. M. S. L. and A. M. T. M. C. acknowledge funding by FEDER, through the COMPETE program, and by FCT (Fundação para a Ciência e a Tecnologia, Portugal), project reference FCOMP-01-0124-FEDER-010787 (FCT PTDC/QUI-QUI/098198/2008). J.M. acknowledges the subsidy by national Portuguese funding through FCT — Fundação para a Ciência e a Tecnologia, projects ref. PEst-OE/EQB/LA0023/2011, and PTDC/QUI-BIQ/112943/2009.

## Appendix A. Supplementary data

*Supplementary data*: time variation of POPC and cholesterol molecular areas for the simulated systems, tilts of POPC P–N and long cholesterol axes relative to the bilayer normal, average transverse positions of selected POPC and cholesterol atoms, pyrene molecules' center of mass and bilayer thickness, lateral mean square displacements' plots of pyrene, POPC and cholesterol and respective lateral diffusion coefficients, rotational autocorrelation functions of several molecular axes in pure POPC and POPC/cholesterol systems (Fig. S1 — S4, Table S1). Supplementary data to this article can be found online at http://dx.doi.org/10.1016/j.bbamem.2012.12.014.

## References

[1] A.P. Lyubartsev, A.L. Rabinovich, Recent development in computer simulations of lipid bilayers, Soft Matter 7 (2011) 25–39.
[2] L.M.S. Loura, J.P. Prates Ramalho, Fluorescent membrane probes' behavior in lipid bilayers: insights from molecular dynamics simulations, Biophys. Rev. 1 (2009) 141–148.
[3] L.M.S. Loura, J.P. Prates Ramalho, Recent developments in molecular dynamics simulations of fluorescent membrane probes, Molecules 16 (2011) 5437–5452.
[4] P. Somerharju, Pyrene-labeled lipids as tools in membrane biophysics and cell biology, Chem. Phys. Lipids 116 (2002) 57–74.
[5] E. Melo, J. Martins, Kinetics of bimolecular reactions in model bilayers and biological membranes. A critical review, Biophys. Chem. 123 (2006) 77–94.
[6] B. Hoff, E. Strandberg, A.S. Ulrich, D.P. Tieleman, C. Posten, $^2$H-NMR study and molecular dynamics simulation of the location, alignment, and mobility of pyrene in POPC bilayers, Biophys. J. 88 (2005) 1818–1827.
[7] J. Martins, E. Melo, Molecular mechanism of lateral diffusion of $py_{10}$-PC and free pyrene in fluid DMPC bilayers, Biophys. J. 80 (2001) 832–840.
[8] M. Herrenbauer, Biosorption of Polycyclic Aromatic Hydrocarbons (PAH) to Microorganisms and Liposomes, Shaker Verlag, Aachen, Germany, 2002.
[9] J. Čurdová, P. Čapková, J. Plášek, J. Repáková, I. Vattulainen, Free pyrene probes in gel and fluid membranes: perspective through atomistic simulations, J. Phys. Chem. B 111 (2007) 3640–3650.
[10] D. Arrais, J. Martins, Bilayer polarity and its thermal dependency in the $\ell_o$ and $\ell_d$ phases of binary phosphatidylcholine/cholesterol mixtures, Biochim. Biophys. Acta 1768 (2007) 2914–2922.
[11] G.P. L'Heureux, M. Fragata, Micropolarities of lipid bilayers and micelles: 5. Localization of pyrene in small unilamellar phosphatidylcholine vesicles, Biophys. Chem. 30 (1988) 293–301.

[12] F. Podo, J.K. Blasie, Nuclear magnetic resonance studies of lecithin bimolecular leaflets with incorporated fluorescent probes, Proc. Natl. Acad. Sci. U. S. A. 74 (1977) 1032–1036.
[13] D. Arrais, J. Martins, Phospholipid/cholesterol binary mixtures: polarity variations with composition and temperature, Eur. Biophys. J. 40 (Suppl. 1) (2011) 195—195.
[14] H.J.C. Berendsen, D. van der Spoel, R. van Drunen, GROMACS: a message-passing parallel molecular dynamics implementation, Comput. Phys. Commun. 91 (1995) 43–56.
[15] E. Lindahl, B. Hess, D. van der Spoel, GROMACS 3.0: a package for molecular simulation and trajectory analysis, J. Mol. Model. 7 (2001) 306–317.
[16] H.J.C. Berendsen, J.P.M. Postma, W.F. van Gunsteren, J. Hermans, Interaction models for water in relation to protein hydration, in: B. Pullman (Ed.), Intermolecular Forces, Reidel, Dordrecht, The Netherlands, 1981, pp. 331–342.
[17] O. Berger, O. Edholm, F. Jahnig, Molecular dynamics simulations of a fluid bilayer of dipalmitoylphosphatidylcholine at full hydration, constant pressure, and constant temperature, Biophys. J. 72 (1997) 2002–2013.
[18] M. Holtje, T. Forster, B. Brandt, T. Engels, W. von Rybinski, H.D. Holtje, Molecular dynamics simulations of stratum corneum lipid models: fatty acids and cholesterol, Biochim. Biophys. Acta 1511 (2001) 156–167.
[19] B. Hoff, Aromaten in Phospholipid-Doppelschichten: molekulardynamische Simulationen und experimentelle Validierung (Ph.D. Thesis), Universitätsverlag Karlsruhe, Karlsruhe, Germany, 2005.
[20] S. Miyamoto, P.A. Kollman, SETTLE: an analytical version of the SHAKE and RATTLE algorithms for rigid water models, J. Comput. Chem. 13 (1992) 952–962.
[21] B. Hess, H. Bekker, H.J.C. Berendsen, J.G.E.M. Fraaije, LINCS: a linear constraint solver for molecular simulations, J. Comput. Chem. 18 (1997) 1463–1472.
[22] K.A. Feenstra, B. Hess, H.J.C. Berendsen, Improving efficiency of large time-scale molecular dynamics simulations of hydrogen-rich systems, J. Comput. Chem. 20 (1999) 786–798.
[23] C. Anézo, C.A.H. de Vries, H.-D. Höltje, D.P. Tieleman, S.-J. Marrink, Methodological issues in lipid bilayer simulations, J. Phys. Chem. B 107 (2003) 9424–9433.
[24] H.J.C. Berendsen, J.P.M. Postma, A. DiNola, J.R. Haak, Molecular dynamics with coupling to an external bath, J. Chem. Phys. 81 (1984) 3684–3690.
[25] U. Essman, L. Perela, M.L. Berkowitz, T. Darden, H. Lee, L.G. Pedersen, A smooth particle mesh Ewald method, J. Chem. Phys. 103 (1995) 8577–8593.
[26] J. Repáková, J.M. Holopainen, M.R. Morrow, M.C. McDonald, P. Čapková, I. Vattulainen, Influence of DPH on the structure and dynamics of a DPPC bilayer, Biophys. J. 88 (2005) 3398–3410.
[27] A.M.T.M. do Canto, A.J. Palace Carvalho, J.P. Prates Ramalho, L.M.S. Loura, Structure and conformation of HIV fusion inhibitor peptide T-1249 in presence of model membranes: a molecular dynamics study, J. Mol. Struct. (THEOCHEM) 946 (2010) 119–124.
[28] A.M.T.M. do Canto, A.J. Palace Carvalho, J.P. Prates Ramalho, L.M.S. Loura, Molecular dynamics simulations of T-20 HIV fusion inhibitor interacting with model membranes, Biophys. Chem. 159 (2011) 275–286.
[29] A.M.T.M. do Canto, A.J. Palace Carvalho, J.P. Prates Ramalho, L.M.S. Loura, Molecular dynamics simulation of HIV fusion inhibitor T-1249: insights on peptide-lipid interaction, Comput. Math. Methods Med. (2012) 151854.
[30] H.A.L. Filipe, M.J. Moreno, L.M.S. Loura, Interaction of 7-nitrobenz-2-oxa-1,3-diazol-4-yl-labeled fatty amines with 1-palmitoyl,2-oleoyl-*sn*-glycero-3-phosphocholine bilayers: a molecular dynamics study, J. Phys. Chem. B 115 (2011) 10109–10119.
[31] H. Flyvbjerg, H.G. Petersen, Error estimates on averages of correlated data, J. Chem. Phys. 91 (1989) 461–466.
[32] W. Humphrey, A. Dalke, K. Schulten, VMD: visual molecular dynamics, J. Mol. Graph. 14 (1996) 33–38.
[33] J. Repáková, P. Čapková, J.M. Holopainen, I. Vattulainen, Distribution, orientation, and dynamics of DPH probes in DPPC bilayer, J. Phys. Chem. B 108 (2004) 13438–13448.
[34] C. Hofsäß, E. Lindahl, O. Edholm, Molecular dynamics simulations of phospholipid bilayers with cholesterol, Biophys. J. 84 (2003) 2192–2206.
[35] M. Alwarawrah, J.A. Dai, J.Y. Huang, A molecular view of the cholesterol condensing effect in DOPC lipid bilayers, J. Phys. Chem. B 114 (2010) 7516–7523.
[36] G. Lantzsch, H. Binder, H. Heerklotz, M. Wendling, G. Klose, Surface areas and packing constraints in POPC/C(12)EO(n) membranes. A time-resolved fluorescence study, Biophys. Chem. 58 (1996) 289–302.
[37] B. Konig, U. Dietrich, G. Klose, Hydration and structural properties of mixed lipid/surfactant model membranes, Langmuir 13 (1997) 525–532.
[38] J.M. Smaby, M.M. Momsen, H.L. Brockman, R.E. Brown, Phosphatidylcholine acyl unsaturation modulates the decrease in interfacial elasticity induced by cholesterol, Biophys. J. 73 (1997) 1492–1505.
[39] R.A. Böckmann, A. Hac, T. Heimburg, H. Grubmuller, Effect of sodium chloride on a lipid bilayer, Biophys. J. 85 (2003) 1647–1655.
[40] P. Mukhopadhyay, H.J. Vogel, D.P. Tieleman, Distribution of pentachlorophenol in phospholipid bilayers: a molecular dynamics study, Biophys. J. 86 (2004) 337–345.
[41] A.A. Gurtovenko, J. Anwar, Interaction of ethanol with biological membranes: the formation of non-bilayer structures within the membrane interior and their significance, J. Phys. Chem. B 113 (2009) 1983–1992.
[42] S.A. Pandit, S.W. Chiu, E. Jakobsson, A. Grama, H.L. Scott, Cholesterol packing around lipids with saturated and unsaturated chains: A simulation study, Langmuir 24 (2008) 6858–6865.
[43] J.P. Douliez, A. Leonard, E.J. Dufourc, Restatement of order parameters in biomembranes: calculation of CC bond order parameters from CD quadrupolar splittings, Biophys. J. 68 (1995) 1727–1739.
[44] D.P. Tieleman, S.J. Marrink, H.J.C. Berendsen, A computer perspective of membranes: molecular dynamics studies of lipid bilayer systems, Biochim. Biophys. Acta 1331 (1997) 235–270.
[45] G. Klose, B. Madler, H. Schafer, K.P. Schneider, Structural characterization of POPC and $C_{12}E_4$ in their mixed membranes at reduced hydration by solid state $^2H$ NMR, J. Phys. Chem. B 103 (1999) 3022–3029.
[46] J. Seelig, N. Waespesarcevic, Molecular order in *cis* and *trans* unsaturated phospholipid bilayers, Biochemistry 17 (1978) 3310–3315.
[47] J.B. Klauda, R.M. Venable, J.A. Freites, J.W. O'Connor, D.J. Tobias, C. Mondragon-Ramirez, I. Vorobyov, A.D. MacKerell, R.W. Pastor, Update of the CHARMM all-atom additive force fields for lipids: validation on six lipid types, J. Phys. Chem. B 114 (2010) 7830–7843.
[48] M. Patra, E. Salonen, E. Terama, I. Vattulainen, R. Faller, B.W. Lee, J. Holopainen, M. Karttunen, Under the influence of alcohol: the effect of ethanol and methanol on lipid bilayers, Biophys. J. 90 (2006) 1121–1135.
[49] A.L. Lomize, I.D. Pogozheva, H.I. Mosberg, Anisotropic solvent model of the lipid bilayer. 2. Energetics of insertion of small molecules, peptides and proteins in membranes, J. Chem. Inf. Model. 51 (2011) 930–946.